1,3-Cycloaddition of Ozone to Ethylene, Benzene, and Phenol: A Comparative ab Initio Study

Marc F. A. Hendrickx* and Chris Vinckier

Department of Chemistry, Katholieke Universiteit Leuven, Celestijnenlaan 200F, B-3001 Leuven, Belgium

Received: March 3, 2003; In Final Form: June 20, 2003

Results of ab initio calculations comparing the 1,3-cycloadditions of ozone to ethylene, benzene, and phenol are presented. The potential energy surfaces of these reactions are explored to establish structures and relative energies of transition states and addition products. Calculations are performed at the B3LYP level for geometry optimizations and at the CCSD(T)/6-31G(d,p) level for energetics. For the ethylene reaction the calculated activation barrier and exothermicity correspond within a few kilocalories per mole with previous theoretical studies and experimental data, rendering credit to the computational model used. Calculations for the benzene ozonolysis yield a barrier of 15.8 kcal/mol that corresponds quite well with the experimental value of 14.6 kcal/mol. The phenol reaction is predicted to possess a barrier of 9.5 kcal/mol. The most stable primary ozonides of benzene and phenol are calculated at 18.9 and 29.0 kcal/mol below the corresponding entrance channels, respectively. In the specific case of the phenol ozonide, the most stable conformation for this intermediate is compatible with the experimentally determined initial reaction product catechol. The carbon rings in the primary ozonides of benzene and phenol are found to retain their planarity.

1. Introduction

Beyond doubt ozone is one of the best known chemical compounds. Its physical and chemical properties are, with respect to mankind, at the same time beneficiary, even essential, and hazardous. The ability of ozone molecules to absorb harmful UV radiation in the Earth's stratosphere is vital for all life on our planet. On the contrary, the strong oxidizing capacity of this compound when present in the troposphere is quite harmful to plants, animals, and humans alike. However, at the level of environmental technology ozone has a large number of practical applications. For instance, ozone has a potential for the purification of industrial wastewaters[1] and is an environmentally friendly alternative for strong oxidizers in the microelectronics industry.[2]

The importance of ozone in atmospheric chemistry is mostly related to its gas-phase reactions with hydrocarbons. It is well established that the chemical lifetime of the so-called volatile organic compounds (VOCs) is determined by their reaction with either ozone or the hydroxyl and nitrate radicals or by photodissociation for molecules containing carbonyl functions.[3] However, due to a complex chain mechanism VOCs in the presence of nitrogen oxides (NO_x) form a reactive mixture which under the influence of sunlight results in a net ozone production cycle. This can quantitatively be expressed for each hydrocarbon by its ozone creation potential (OCP).[4] As a result of the higher precursor emissions over the years, one sees a continuous increase of the troposheric ozone background concentration since preindustrial times.[5] In addition the ozone air quality guidance level of 120 μg m^{-3} for the protection of human health, as accepted by the World Meteorological Organisation (WMO), is exceeded several days a year during the summer period in many countries.[6] Besides being a very powerful oxidizer, ozone is also considered a relatively important greenhouse gas.[7]

One well-established strategy of bringing down troposheric ozone is by reducing both the VOC and NO_x emissions. The magnitude of this reduction of, e.g., the VOCs, can be estimated by air quality simulation models such as the regional atmospheric chemistry mechanism (RACM)[8] or the master chemical mechanism (MCM).[9] In these models the initial reaction step with ozone involves essentially alkenes and aromatics, since they contain unsaturated carbon bonds that are the preferred sites for ozone addition. In this context ethylene and the simple aromatics toluene, xylenes, and benzene are considered as model VOCs in view of their large OCP values.[4]

In addition to the importance of ozone reactions in the gas phase, a relatively new domain is the application of ozonated aqueous solutions to remove organic pollutants from wastewaters and process waters by advanced oxidation processes (AOPs).[1] This technique seems very suitable to break down organic pollutants such as recalcitrant aromatic compounds to smaller oxygenated and more water soluble fragments. In this way biologically degradable molecules are formed which can be eliminated in conventional biological water purification systems.[10] These AOPs are more environmentally friendly than the strong oxidizers such as permanganate, chromate, or chlorine and will be applied in the future in many industrial sectors in the frame of the implementation of the concepts of sustainable chemistry. Molecules of high relevance in this context are those containing aromatic ring structures such as the phenolic compounds.

An excellent evaluation of the kinetic parameters of the ozone reactions in the gas phase for numerous classes of hydrocarbons is given in a compilation assembled by R. Atkinson.[11] A striking observation is that one sees a tremendous decrease of the reactivity when going from ethylene to the simple aromatic molecules. Indeed, kinetic measurements have shown that the Arrhenius activation energies E_a for the ozone reactions increase as E_a(ethylene) = 5.1 kcal/mol $\ll$ E_a(toluene) = 13.2 kcal/mol and E_a(benzene) = 14.6 kcal/mol. When reactions in the liquid phase are considered, large differences within the class of the

10.1021/jp034541x CCC: $25.00
Published on Web 08/23/2003

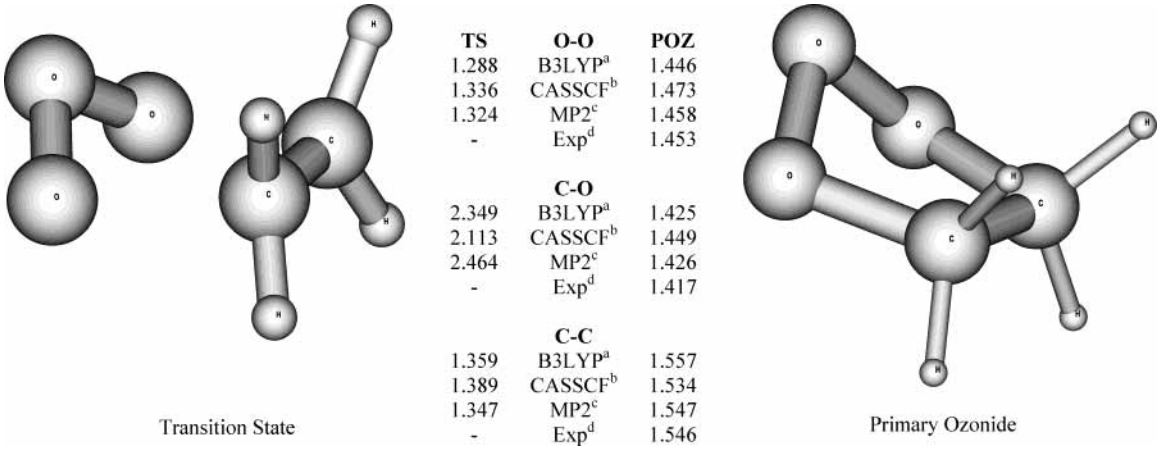

TS	O-O	POZ
1.288	B3LYP[a]	1.446
1.336	CASSCF[b]	1.473
1.324	MP2[c]	1.458
-	Exp[d]	1.453
	C-O	
2.349	B3LYP[a]	1.425
2.113	CASSCF[b]	1.449
2.464	MP2[c]	1.426
-	Exp[d]	1.417
	C-C	
1.359	B3LYP[a]	1.557
1.389	CASSCF[b]	1.534
1.347	MP2[c]	1.547
-	Exp[d]	1.546

Figure 1. 1,3-Cycloaddition of ozone on ethylene: B3LYP geometries of the transition state and the primary ozonide. Bond distances are given in angstroms. Superscript letters a−d indicate this work, CASSCF geometries of ref 23, MP2 geometry of ref 19, and experimental geometry of refs 17 and 18, respectively.

aromatic compounds are measured: E_a(benzene) = 21 kcal/mol ≫ E_a(phenol) = 5.5 kcal/mol.[12]

Although the ozonolysis of different compounds is currently receiving a lot of attention,[13−16] a very interesting and yet unresolved question concerns the underlying mechanisms that are to be held responsible for this wide range of observed activation energies. In this paper transition states for the relatively simple model compounds ethylene, benzene, and phenol in their reaction with ozone will be determined and the heights of the reaction barriers calculated. It will be shown that the observed trends in reactivity can be explained in terms of simple properties of these molecules. The calculated relative stabilities of the various addition products for the phenol reaction will be compared and confronted with the experimental fact that catechol has been identified as an initial reaction product. A detailed analysis of the geometries of the stationary points on the potential energy surfaces is given.

2. Computational Model

The addition of ozone on ethylene has been studied in the past both experimentally[17,18] and theoretically. Extensive calculations have been performed in the past[19−23] to determine the binding energy of the primary ozonide and the height of the energy barrier in the entrance channel. The results of these accurate calculations can therefore be combined with the corresponding experimental value to provide a reference value for our benchmark calculations on this system. The aim is to arrive at a computational model that gives reliable results for the ethylene reaction and still is applicable to the phenol case. After several test calculations involving different methods for obtaining the relative energies of various stationary points on the potential energy surface and for performing geometry optimizations, we found the following model to be a good tradeoff between accuracy and computational demand. The 6-31G(d,p) basis set is used throughout. Polarization functions on the hydrogen atoms are necessary because in some structures the hydroxyl hydrogen plays a more or less critical role in their relative stabilities. Full geometry optimizations were performed at the B3LYP level by using gradient techniques. At the same level of computation all stationary points were characterized as either a minimum or a transition state by performing harmonic vibrational analyses using analytical second derivatives. We will demonstrate that reliable and sufficiently accurate energetics for the systems at hand are only achievable by using a wave function computational technique. Final estimates for the relative energies of the various stationary points are made by carrying out CCSD(T) calculations for which only the inner core electrons are excluded from the correlation treatment. The GAUSSIAN 98[24] software was used to perform all the calculations.

3. Results and Discussion

3.1. Reaction of Ozone with Ethylene. Recently, the complete reaction mechanism of the ozonolysis of ethylene[23] and acetylene[25,26] has been described theoretically in great detail.[27,28] Even for the simplest case of the olefins (ethylene), the formation of these final reaction products appears to be very complex, involving more than 40 relevant conformations. Despite this rather complex reaction mechanism, one important and surprisingly simple conclusion could be drawn from this ab initio study. It appeared that the initial addition of O_3 to the double bond of the ethylene molecule is the rate-determining step of the overall oxidation process.

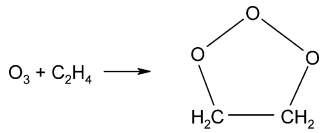

This can be understood from (i) the fact that the 1,2,3-trioxolane (Figure 1), which is also known as molozonide or primary ozonide (POZ), is situated experimentally 45 ± 6 kcal/mol below the reactants and (ii) the large exothermicity of the complete ozonolysis process. Consequently, the transition state leading to this intermediate is responsible for the overall reaction rate of the oxidation process. As a first step in the study of the ozonolysis of ethylene, benzene, and phenol, it is thus logical to confine our calculations to the structures involved in the 1,3-cycloaddition.

In a previous detailed theoretical studiy[19] it was found that, during the early stages of the addition of ozone to ethylene, a weakly bound van der Waals (VDW) complex is formed. For these complexes various structures were considered by the authors, i.e., one or two oxygen atoms bound to one or two hydrogen atoms and one or two oxygen atoms bound to the π system of ethylene. Of all the structures considered the most stable one was found to have a stability of only 0.4 kcal/mol at the MP4 level after correction for the zero-point vibrational energy. A later study[21] confirmed these findings in the sense that these complexes lie in a shallow minimum 0.74 kcal/mol

TABLE 1: 1,3-Cycloaddition of Ozone on Ethylene[a]

	B3LYP (6-31G(d,p))		CCSD (T) (6-31 G(d,p))		ref 19 MP4 (6-31G(d,p))	ref 23 CCSD(T) (6-31G(2d,2p))	
ethylene + ozone	ΔE_e	+ZPE	ΔE_e	+ZPE	ΔE_e + ZPE	ΔE_e + ZPE	expt[17,18]
reactants	0	0	0	0	0	0	0
transition state	−3.1	−1.4	1.6	3.3	2.5	5.0	5.0
primary ozonide	−62.3	−57.3	−57.5	−52.5	−46.0	−49.2	−45 ± 6

[a] Relative energies in kcal/mol of the various stationary points; comparison with previous calculations and experiment.

below the reactants. The addition reaction then proceeds by a transition state that is calculated 2.5 kcal/mol above the entrance channel in ref 19. More recent theoretical studies[22,23] all find small activation energies for this ozonolysis reaction, the latest[23] reporting a value that corresponds exactly with the experimental activation energy of 5 kcal/mol. All possible conformations of the addition product POZ were described in great detail.[19] It was found from MP2 geometry optimizations that the so-called O-envelope (the two carbon atoms and the two terminal oxygen atoms of ozone are located in the same plane, and the remaining oxygen atom is located out of the plane, as illustrated in Figure 1) is the only stable cyclic addition product, a theoretical finding that agrees with the experimental microwave structure.[17,18] The two other candidates, namely, the C-envelope (the three oxygen atoms and one carbon atom coplanar, one carbon atom out-of-plane) and the O-adjacent-envelope (two carbons, the middle oxygen, and one terminal oxygen of ozone coplanar) do not represent a stable intermediate on the potential energy surface since structures of this type collapsed without an energy barrier to the O-envelope.

From the above it is clear that the most favorable reaction path for the 1,3-cycloaddition of ozone on ethylene passes through an O-envelope-shaped VDW complex and transition state, producing a POZ of the same structure. Since the VDW complex is of little importance for the observed reactivity, we will only discuss the B3LYP geometries for the latter two structures, which were characterized by this computational technique as stationary points on the potential energy surface. Their relative energies and a comparison with previous calculations can be found in Table 1, where the CSSD(T) energies are calculated at the B3LYP geometries. Graphical representations of the B3LYP transition structure and primary ozonide are depicted in Figure 1, which also compares the bond distances obtained for the different computational techniques. For the POZ the correspondence between the MP2 geometry and the experimental bond distances is good. The deviations for O−O, C−C, and C−O distances remain limited to a maximum of 0.009 Å for the C−O bond, while the CASSCF geometry given in ref 23 differs much more from the experimental data. Again the C−O bond turns out to exhibit the largest deviation since it is calculated too long by as much as 0.032 Å. Our B3LYP POZ structure on the contrary resembles much better the experimental structure and consequently the MP2 result. Differences between the three sets of data are limited to about 1/100 Å. The different result for CASSCF can most probably be attributed to this computational method itself. Indeed, the 6-31G(d) basis set employed in the CASSCF study differs only from the 6-31G-(d,p) basis sets used for the MP2 and our B3LYP calculations in the presence of a polarization function on the hydrogen atoms and is therefore most likely not to influence the bond distances between the heavy atoms C and O. A comparison of the geometrical data for the transition state is also given in Figure 1. Again the MP2 and B3LYP methods give comparable structures, while the CASSCF geometry for the transition state (TS) deviates the most. The deviations are however more pronounced than in the case of the POZ intermediate. This reflects the looser geometric and consequently electronic structure of the transition state. The C−O distance which controls the approach of the reactants appears to be the most affected; the deviation of the CASSCF distance from MP2 and B3LYP values amounts to as much as several tenths of an angstrom. Our B3LYP transition state as shown in Figure 1 reveals that the O_3 and ethylene moieties resemble very well the reactants; i.e., the O−O bond distance of 1.288 Å is only marginally larger than its ozone value of 1.265 Å, and the C_2H_4 part is still quite flat. We can therefore safely conclude that the system reaches its TS during the early stages of the 1,3-cycloaddition, closely after the formation of the VDW complex.

Consequently, one may expect the activation energy for the ozonolysis of ethylene to be quite small. As can be deduced from Table 1 this indeed appears to be the case. At the B3LYP level the electronic energy difference ΔE_e between the reactants and the transition state is −3.1 kcal/mol, indicating that the latter structure is even positioned energetically below the reactants and just slightly above the VDW complex. Even after correction for the zero-point vibration energy the barrier between the complex and the POZ is still situated lower than the reactants at −1.4 kcal/mol (Table 1). Carrying out CCSD(T) calculations using the B3LYP geometries raises the level of the transition state above the entrance channel to 3.3 kcal/mol, a finding comparable to the MP4 result of 2.5 kcal/mol and almost within chemical accuracy (1 kcal/mol) of the experimental value of 5 kcal/mol. Further on, our computational model also reproduces the large exothermicity of this cycloaddition reaction. Our final CCSD(T) estimate of 52.5 kcal/mol falls only by about 1.5 kcal/mol outside the experimental range of 45 ± 6 kcal/mol. In addition, a more advanced theoretical treatment[23] yields a value of about 49 kcal/mol, which is close to the upper limit of the experimental range and only about 3.5 kcal/mol different from our result. In view of the foregoing, it is appropriate to use the same computational methodology for our study of the ozonolysis of benzene and phenol. As a final remark concerning this reaction, we mention that the B3LYP method gives acceptable results for the geometries of the stationary points but relative energies that are somewhat less accurate than those of CCSD-(T). The deviations amount to about 5 and 8 kcal/mol when compared to the CCSD(T) values and the experimental values, respectively.

3.2. Reaction of Ozone with Benzene. To date and to our knowledge the addition of ozone to benzene has only been studied on an experimental basis;[11] no theoretical study has been reported in the literature so far. From preliminary calculations it was deduced that this reaction proceeds in a concerted fashion. In this case the addition can occur on two carbon atoms in the α, β, or γ position of each other; the α addition is found to produce POZ structures that are by far the most stable. The reason for this can most probably be attributed to a 1,3-butadiene-like moiety, which is only present in the product of the α addition. Optimization of the γ structure yields a local minimum on the potential energy surface that is at the CCSD-(T) level 15 kcal/mol higher than the α-POZ. A detailed search did not yield a stable structure in which the ozone molecule is

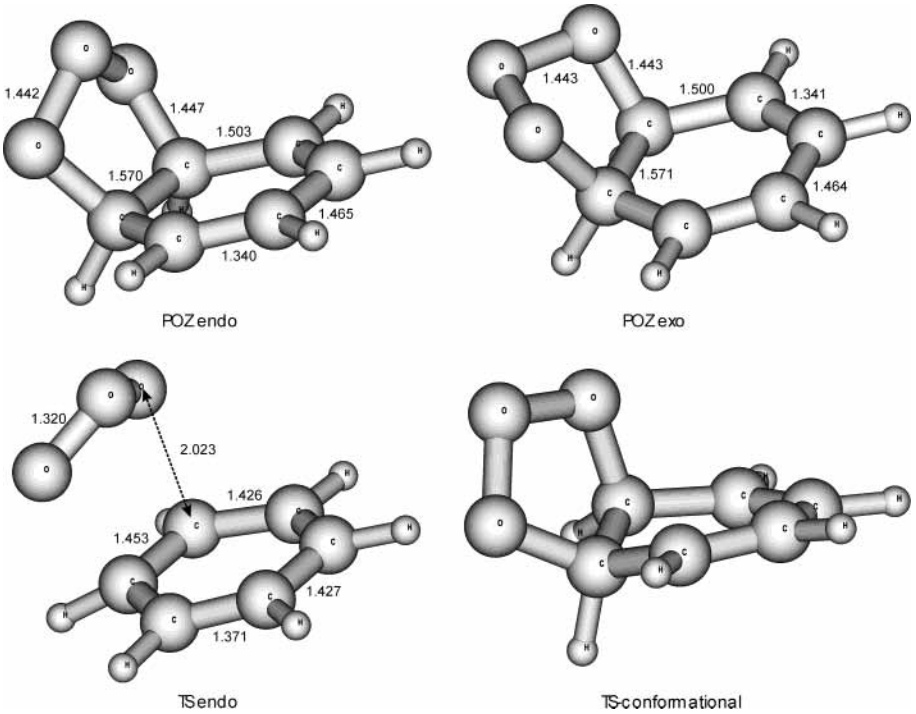

Figure 2. 1,3-Cycloaddition of ozone on benzene: B3LYP geometries for various stationary points. All distances are given in angstroms.

TABLE 2: 1,3-Cycloaddition of Ozone on Benzene[a]

		B3LYP (6-31G(d,p))		CCSD(T) (6-31G(d,p))	
benzene + ozone		ΔE_e	+ZPE	ΔE_e	+ZPE
	reactants	0	0	0	0
endo	TS	7.2	8.3	14.7	15.8
	POZ	−23.3	−20.5	−21.5	−18.6
exo	TS	9.8	10.7	17.0	17.9
	POZ	−23.4	−20.6	−21.8	−18.9

[a] Relative B3LYP and CCSD(T) electronic energies ΔE_e. Zero-point vibrational energies (+ZPE) calculated with B3LYP. All values in kcal/mol.

bound to two carbon atoms that are in β position with respect to each other. All attempts collapsed to either α- or γ-POZ. Even if our study is confined to the α type addition, still two mechanistically different approaches need to be considered: the middle oxygen atom of ozone is either directed toward the benzene ring or directed away from this ring structure. The former reaction path results in an *endo*-type transition state and primary ozonide, whereas for the latter approach similar conformations of an *exo* type must be examined. The resulting B3LYP geometries are depicted in Figure 2 and the relative energies collected in Table 2. From this table it can be concluded that at the B3LYP and CCSD(T) levels the energetic positions of the two conformers of the POZ are nearly identical, the difference being less than 1/2 kcal/mol. Our calculations arrive at an exothermicity of about −19 kcal/mol, an absolute value much smaller than the one obtained for the ethylene/ozone system.

With the purpose of getting an idea of the energy barrier separating these two isomers, the transition state connecting them was located on the potential energy surface. A graphical representation of this structure, denoted as TS-conformational, is shown in Figure 2. In contrast to the POZ structures the transition state has a somewhat twisted conformation in the sense that the C_6 ring is not planar and that the two C−O bonds are no longer coplanar. The barrier height with respect to the lowest POZ and after correction for the zero-point vibration energy was calculated at 3.5 and 3.0 kcal/mol at the B3LYP and CCSD-

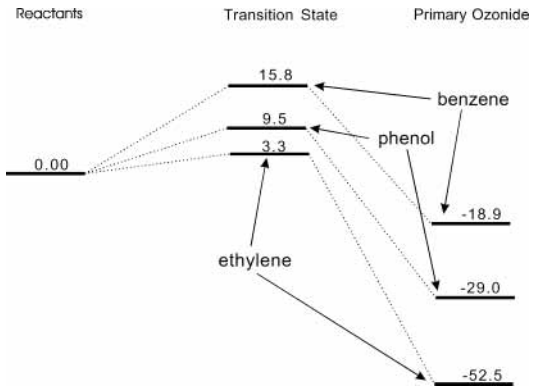

Figure 3. Comparison of the activation barriers (kcal/mol) and exothermicities of the 1,3-cycloadditions of ozone on ethylene, benzene, and phenol.

(T) levels, respectively. Therefore, even at room temperature, there is a dynamical equilibrium between these two conformational isomers. The transition state in the entrance channel between the VWD complex and the POZ on the contrary lies considerably higher. Although the most favorable reaction path is clearly the one involving the *endo*-type transition state, the difference between the two additions is quite small, only 2.1 kcal/mol at the CCSD(T) level. Table 2 shows however that there is a substantial difference between B3LYP and CCSD(T) concerning the actual calculated barrier heights. Even though activation barriers in the latter case are obtained by using the B3LYP-optimized geometries, a deviation of more than 7 kcal/mol is found. In view of the better results obtained by the CCSD(T) wave function technique for the ethylene/ozone system, we propose 15.8 kcal/mol as our final estimate for the activation barrier of the 1,3-cycloaddition of ozone to benzene. This value is in excellent agreement with the experimental value of 14.6 kcal/mol.[11] As shown in Figure 3, which contains a comparison for the different ozone reactions presently studied, the reaction of benzene is predicted to be much slower than the ethylene reaction, a theoretical conclusion that is confirmed by measured reaction rates. Most probably the loss of aromaticity

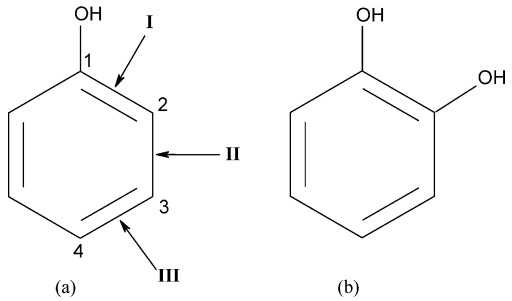

Figure 4. (a) 1,3-Cycloaddition of ozone on phenol: schematic representation of the three modes of addition. (b) Structure of the initial reaction product catechol.

in the case of benzene is responsible for this different behavior between the two molecules, since both π systems react in a mechanistically similar fashion.

Both POZ structures shown in Figure 2 possess a planar carbon ring structure. From the bond distances between the four carbon atoms that are not bound to oxygen, a 1,3-butadiene-like moiety can be deduced, which explains the planar arrangement of the carbon ring. Indeed, two double CC bonds exhibiting bond distances of about 1.34 Å enclose a single CC bond of 1.465 Å. The remaining three CC bonds are single bonds with a bond length of 1.5 Å or larger. Surely, these results are in agreement with qualitative and obvious considerations that can be made for these molecules, and therefore render credit to the reliability of our ab initio calculations. Similar observations, although definitely less pronounced, can be made for the *endo* transition state in Figure 2. This indicates that the incoming ozone molecule has to some extent destroyed the aromatic character of the benzene part. The planar conformation of the carbon ring structure and the attached hydrogen atoms remains however largely intact, suggesting again that the transition state is reached at an early stage of the reaction.

3.3. Reaction of Ozone with Phenol. The addition of ozone to phenol can occur in many ways, but from the foregoing calculations on benzene it follows that the most stable structures of the POZ are those for which the cycloaddition takes place at two neighboring carbon atoms of the aryl ring. In this case the incoming ozone can attach at three distinct places as is shown in Figure 4: an addition at positions 1 and 2, at positions 2 and 3, or at positions 3 and 4. In the following we will describe these three addition paths as modes I, II, and III, respectively. Moreover, the direction of the hydroxyl group with respect to the incoming ozone gives two possibilities: the hydrogen atom of this group can be oriented either toward or away from the ozone. We will denote the resulting reactions as *endo*-H or *exo*-H, respectively. Finally, the middle oxygen of ozone can be oriented toward (*endo*-O) or away (*exo*-O) from the aryl ring. In total we need therefore to consider 12 possible modes of reactions. Transition states and POZ for all these 12 cycloadditions have been located at the B3LYP level and their relative energies estimated with CCSD(T). The corresponding relative energies are presented in Table 3. In accordance with the ethylene and benzene reaction, the B3LYP energies are only in qualitative agreement with the computationally more expensive CCSD(T) method. Since the activation barriers and the bond energies for these benchmark reactions are calculated to be too small by about 5 kcal/mol by B3LYP (Tables 1 and 2), the use of CCSD(T) is a necessity for obtaining reliable results.

All primary ozonides are positioned at energies lower than 20 kcal/mol below the reactants. The largest stabilities are found for these structures where the ozone is bound to the two carbon atoms in the immediate vicinity of the hydroxyl group of phenol (path I). The most stable structures have bond energies of about 29 kcal/mol and possess geometries exhibiting an *exo*-O conformation with the hydroxyl hydrogen in either the *exo* or *endo* position. Both these POZs are depicted in the lower part of Figure 5. Paths II and III produce POZs that are situated on the average about 22−23 kcal/mol below the entrance channel. The energy difference between the least and most stable structures is predicted to be 7.8 kcal/mol. For the transition states the lowest activation barrier of 9.5 kcal/mol is found again for the mode I approach with both the ozone oxygen and the hydroxyl hydrogen in the *endo* position (Figure 5). The calculated range of activation barriers of 5.0 kcal/mol is smaller than that of the bond energies. Nevertheless, the mode I approach is energetically the most favorable, and one can expect it to be the major reaction path at room temperature. This confirms the finding that catechol (Figure 4) is shown to be an initial product.[27,28] Indeed, after the cycloaddition the hydrogen atom can shift from carbon number 2 (Figure 4) to the neighboring oxygen atom with the expulsion of an O_2 molecule. To prove this fact rigorously, more calculations, involving solvent effects and a mechanism for the O_2 loss, are needed. This will be the subject of our further investigations. In comparison with the benzene ozonlysis our calculations predict that the phenol should react considerably faster, the difference in activation barrier exceeding 6 kcal/mol (Figure 3), a prediction that is in accordance with experimental data.[12] Both the increased reactivity of phenol in comparison with benzene and the preferred addition of ozone in the vicinity of the hydroxyl group (mode I) can be explained in terms of the electrical charges on the carbon atoms of the aryl ring and the oxygen atoms of ozone. Indeed, a Mulliken population analysis clearly shows that the terminal oxygen atoms of ozone are negatively charged (-0.15 e$^-$), a result also found in ref 21. Due to the larger electronegativity of carbon with respect to hydrogen, the carbon atoms of benzene are calculated to have a negative charge of -0.15 e$^-$. The electron-withdrawing capacity of the hydroxyl group of phenol causes the carbon atom bound to this group (C_1 in Figure 4a) to have a Mulliken charge that is positive by as much as $+0.32$ e$^-$, whereas the other carbon atoms of phenol remain slightly negatively charged (~ -0.10 e$^-$). This reduced value in comparison with that of benzene explains the overall increased reactivity of phenol toward ozone. The attractive electrostatic forces between C_1 and the terminal oxygen atoms of ozone make addition mode I the most favorable one.

From the geometries as shown in Figure 5 conclusions similar to those for the benzene addition can be drawn. The most obvious characteristic is the conservation of the planar structure of the aryl ring. In comparison with the phenol geometry, also given in Figure 5, the C−C distances in the carbon ring in both POZ conformations are either significantly shorter or significantly larger. This indicates the destruction of the aromaticity and the presence of two double bonds separated by single C−C bonds. It is the presence of a 1,3-butadiene moiety that keeps the carbon ring planar. The C−O distance of the hydroxyl group elongates from a value of 1.368 Å for phenol to about 1.40 Å for both POZ conformations. This reflects the fact that the conjugation effect of the hydroxyl group with the π system of the phenyl ring is no longer active in the POZ. The minute elongations calculated point to an extremely small conjugation effect in the free phenol.

4. Conclusion

For the 1,3-cycloaddition of ozone to ethylene our computational model, which comprises B3LYP geometry optimizations

TABLE 3: 1,3-Cycloaddition of Ozone on Phenol[a]

			transition state		primary ozonide	
			B3LYP ΔE_e + ZPE	CCSD(T) ΔE_e + ZPE	B3LYP ΔE_e + ZPE	CCSD(T) ΔE_e + ZPE
1,2-addition, mode I	*endo*-O	*endo*-H	5.1	9.5	−23.5	−27.1
		exo-H	6.8	11.2	−21.7	−24.8
	exo-O	*endo*-H	8.5	12.2	−24.9	−29.0
		exo-H	8.7	12.2	−24.9	−28.7
2,3-addition, mode II	*endo*-O	*endo*-H	7.9	12.5	−22.3	−23.3
		exo-H	8.1	12.6	−21.7	−22.6
	exo-O	*endo*-H	9.9	14.4	−22.9	−23.8
		exo-H	10.1	14.4	−21.7	−22.6
3,4-addition, mode III	*endo*-O	*endo*-H	6.2	11.3	−22.2	−23.3
		exo-H	7.2	12.4	−20.3	−21.2
	exo-O	*endo*-H	8.6	13.4	−22.6	−23.8
		exo-H	9.6	14.5	−20.8	−21.8

[a] Relative B3LYP and CCSD(T) electronic energies ΔE_e. Zero-point vibrational energies (+ZPE) calculated with B3LYP. All values in kcal/mol.

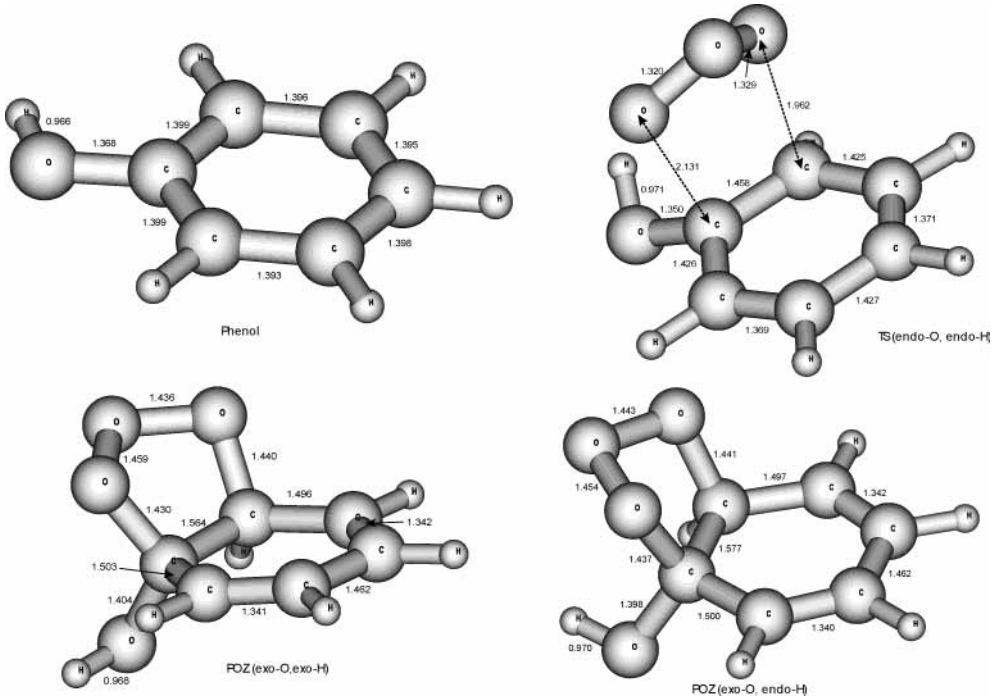

Figure 5. 1,3-Cycloaddition of ozone on phenol: B3LYP geometries for phenol, the most favorable transition state, and the most favorable POZ intermediates. All distances are given in angstroms.

and single-point CCSD(T) calculations, yields activation barrier heights and relative energies for the primary ozonides that are in reasonable agreement with previous calculations and experimental data. Applying the same computational model to the benzene and phenol reactions resulted in activation energies of 15.8 and 9.5 kcal/mol and exothermicities of 18.9 and 29.0 kcal/mol, respectively. From these values it is immediately clear that for an addition of ozone to a particular π system there is a distinct correlation between the barrier height and the extent of the exothermicity. The highest bond energy and the lowest barrier are found for the ethylene addition, whereas addition to benzene requires the largest activation energy and is the least exothermic reaction. Obviously, the reason for this result is the loss of aromaticity of the carbon ring, which destabilizes the primary ozonide by more than 30 kcal/mol. On the contrary, the presence of a hydroxyl group on the phenyl ring unambiguously assists the addition by a drop of the activation energy of more than 6 kcal/mol. An explanation in terms of electrostatic interactions between the reactants is given. The calculated activation energy for benzene is in excellent agreement with its experimental gas-phase value of 14.6 kcal/mol. For reactions in aqueous solutions, the increased reactivity of phenol in comparison with benzene as found experimentally is qualitatively reproduced by our calculations. The addition of ozone in the immediate vicinity of the hydroxyl group (mode I) is found to be the most favorable approach for phenol and agrees with the empirical fact that catechol is an initial product for this oxidation process.

Acknowledgment. Financial support by the Belgian National Science Foundation and the Flemish Government under the Concerted Action Scheme are gratefully acknowledged.

References and Notes

(1) Gunukula, R. V. B.; Tittlebaum, M. E. *J. Environ. Sci. Health, Part A* **2001**, *36*, 307.

(2) Jeon, J. S.; Ogle, B.; Bayens, M.; Mertens, P. *Solid State Phenom.* **1999**, *65*−*66*, 119.

(3) Finlayson-Pittsand, B. J.; Pitts, J. N., Jr. *Atmospheric Chemistry*; J. Wiley & Sons: New York, 1986; p 405.

(4) Derwent, R. G.; Jenkin, M. E.; Saunders, S. M.; Pilling, M. J. *Atmos. Environ.* **1998**, *32*, 2429.

(5) Wayne, R. P. *Chemistry of the Atmospheres*; Oxford University Press: Oxford, U.K., 2000; p 401.

(6) *Europe's Environment: the Second Assessment*; Elsevier Science Ltd.: Oxford, U.K., 1998; p 98.

(7) *Climate Change 2001: The Scientific Basis*; Houghton, J. T., et al., Eds.; Cambridge University Press: Cambridge, U.K., 2001; p 8.

(8) Stockwell, W. R.; Kirchner, F.; Kuhn, M. *J. Geophys. Res.* **1997**, *102*, 25847.

(9) CAST website http://www.chem.leeds.ac.uk/Atmospheric/MCM/main.html#Master.

(10) Ledakowics, S.; Solecka, M. *Water Sci. Technol.* **2000**, *41*, 157.

(11) Atkinson, R. Gas-Phase Tropospheric Chemistry of Organic Compunds. *Journal of Physical and Chemical Reference Data*; American Institute of Physics: Melville, NY, 1994; Monograph No. 2.

(12) Website of The Radiation Chemistry Data Center of the Notre Dame Radiation Laboratory: http://www.rcdc.nd.edu/Solnkin1/.

(13) Gutbrod, R.; Kraka, E.; Schindler, R. N.; Cremer, D. *J. Am. Chem. Soc.* **1997**, *119*, 7330.

(14) Gutbrod, R.; Schindler, R. N.; Kraka, E.; Cremer, D. *Chem. Phys. Lett.* **1996**, *252*, 221.

(15) Kraka, E.; Cremer, D.; Koller, J.; Plesnicar, B. *J. Am. Chem. Soc.* **2002**, *124*, 8462.

(16) Plescinar, B.; Cerkovnik, J.; Tuttle, T.; Kraka, E.; Cremer, D. *J. Am. Chem. Soc.* **2002**, *124*, 11260.

(17) Zozom, J.; Gillies, C. W.; Suenram, R. D.; Lovas, F. J. *Chem. Phys. Lett.* **1987**, *139*, 64.

(18) Gillies, J. Z.; Gillies, C. W.; Suenram, R. D.; Lovas, F. J. *J. Am. Chem. Soc.* **1988**, *110*, 7991.

(19) McKee, M. L.; Rohlfing, C. M. *J. Am. Chem. Soc.* **1989**, *111*, 2497.

(20) Cremer, D. *J. Am. Chem. Soc.* **1981**, *103*, 3627.

(21) Gillies, C. W.; Gillies, J. Z.; Suenram, R. D.; Lovas, F. J.; Kraka, E.; Cremer, D. *J. Am. Chem. Soc.* **1991**, *113*, 2412.

(22) Olzmann, M.; Kraka, E.; Cremer, D.; Gutbrod, R.; Andersson, S. *J. Chem. Phys.* **1997**, *101*, 9421.

(23) Anglada, J. M.; Crehuet, R.; Bofill, J. M. *Chem.—Eur. J.* **1999**, *5*, 1809.

(24) Frisch, M. J.; Trucks, G. W.; Schlegel, H. B.; Scuseria, G. E.; Robb, M. A.; Cheeseman, J. R.; Zakrzewski, V. G.; Montgomery, J. A., Jr.; Stratmann, R. E.; Burant, J. C.; Dapprich, S.; Millam, J. M.; Daniels, A. D.; Kudin, K. N.; Strain, M. C.; Farkas, O.; Tomasi, J.; Barone, V.; Cossi, M.; Cammi, R.; Mennucci, B.; Pomelli, C.; Adamo, C.; Clifford, S.; Ochterski, J.; Petersson, G. A.; Ayala, P. Y.; Cui, Q.; Morokuma, K.; Malick, D. K.; Rabuck, A. D.; Raghavachari, K.; Foresman, J. B.; Cioslowski, J.; Ortiz, J. V.; Baboul, A. G.; Stefanov, B. B.; Liu, G.; Liashenko, A.; Piskorz, P.; Komaromi, I.; Gomperts, R.; Martin, R. L.; Fox, D. J.; Keith, T.; Al-Laham, M. A.; Peng, C. Y.; Nanayakkara, A.; Challacombe, M.; Gill, P. M. W.; Johnson, B.; Chen, W.; Wong, M. W.; Andres, J. L.; Gonzalez, C.; Head-Gordon, M.; Replogle, E. S.; Pople, J. A. *Gaussian 98*, Revision A.9; Gaussian, Inc.: Pittsburgh, PA, 1998.

(25) Cremer, D.; Kraka, E.; Crehuet, R.; Angada, J.; Gräfenstein, J. *Chem. Phys. Lett.* **2001**, *347*, 268.

(26) Cremer, D.; Crehuet, R.; Anglada, J. *J. Am. Chem. Soc.* **2001**, *123*, 6127.

(27) Bailey, P. S. In *Ozonation in Organic Chemistry*; Blomquist, A. T., Wasserman, H. H., Eds.; Academic Press: New York, 1982; Vol. I.

(28) Singer, P. C.; Gurol, M. D. *Water Res.* **1983**, *17*, 1163.